Horizontal Deflection of Acoustic Paths by Mesoscale Eddies

WALTER H. MUNK

Scripps Institution of Oceanography, University of California, San Diego, La Jolla 92093

(Manuscript received 7 August 1979, in final form 10 December 1979)

ABSTRACT

The horizontal angular deflection of a ray path through a circular eddy is roughly 2ν, where ν is the fractional variation in sound speed at the eddy center; ν may reach 0.03 for intense Gulf Stream rings but is typically < 0.01 for mesoscale eddies. A critical parameter is the ratio $\sigma = \nu R/r$ of acoustic range R to the "eddy focal length" r/ν, where r is the eddy radius. Rays are split into horizontal multipaths for $\sigma > 1$. However, even for very intense rings at extreme ranges, we have $\sigma < 1$, and generally $\sigma \ll 1$. Simple formulas are given for the horizontal deflection and for the perturbations in intensity and in travel time due to an eddy passing between source and receiver. Signatures of cold and warm core rings differ markedly because of differences in eddy dynamics, as well as differences in acoustic propagation properties. Fine-structure associated with internal waves induces a slight spread in the acoustic beam; the horizontal spread is of the same order as the horizontal deflection from mesoscale eddies.

1. Introduction

In a recent paper, Munk and Wunsch (1979) have proposed that the oceans could be mapped to mesoscale resolution by measuring fluctuations in acoustic travel time between a number of distributed transmitters and receivers. The paths were assumed to remain in the vertical plane through the transmitter and receiver. Yet it is well-known that horizontal gradients in sound speed cause horizontal deflections in ray paths. Similarly, waves reflected from sloping bottom boundaries are horizontally deflected (Harrison, 1977). But I am concerned here not with the mean situation, for which (at least in principle) the appropriate azimuth corrections could be worked out, but with departures caused by transient ocean features. Here the mesoscale eddies and their powerful cousins, the Gulf Stream rings, are probably the important features.

The derivation is restricted to a fixed horizontal plane (as for the axial ray) to avoid the complexity of the three-dimensional refraction problem. I believe this procedure is a reasonable way to get at the magnitudes involved, but will eventually have to be tested by a three-dimensional treatment.

2. Ray paths

The differential equation of a ray path in cylindrical coordinates is (Fig. 1)

$$\tan\alpha = \frac{dr}{rd\mu}. \tag{1}$$

Snell's law in cylindrical coordinates for a cylindrically layered medium can be written (see the Appendix)

$$rn(r)\cos\alpha(r) = r_1 n_1 = r_0\cos\alpha_0, \tag{2}$$

where $n(r) = C_0/C(r)$ is the index of refraction referred to conditions outside the eddy. This gives $dr/r = \tan\alpha d\alpha - dn/n$; from (1) we then have

$$\mu = \int_0^\alpha d\alpha - \int_{n_1}^n \frac{dn}{n}\frac{1}{\tan\alpha} = \alpha - \int_{n_1}^n \frac{dn}{n}\frac{1}{\tan\alpha}, \tag{3}$$

since $\alpha(n_1) = 0$. The turning angle θ is then

$$\theta = \mu - \alpha = -\int_{n_1}^n \frac{dn}{n}\frac{1}{\tan\alpha}. \tag{4}$$

For a specified $n(r)$, together with Snell's law for $n(r,\alpha)$ from Eq. (2), one can derive $n(\alpha)$, and integrate (4) from $\alpha(n_1) = 0$ to $\alpha(n)$. In particular, $\alpha(n_0) = \alpha_0$ gives the "exit angle" θ_0. The ray is deflected by the eddy through an angle $2\theta_0$.

3. Weak "scattering"

We take the simple case of linear $n(r)$

$$n = 1 + \nu\frac{r_0 - r}{r_0}, \quad \nu \ll 1, \tag{5}$$

for $r \leqslant r_0$, and $n = 1$ for $r > r_0$. From (2), $r = r_0 \times \cos\alpha_0/\cos\alpha(r) + \text{order}(\nu)$, and so

0022-3670/80/040596-09$06.25

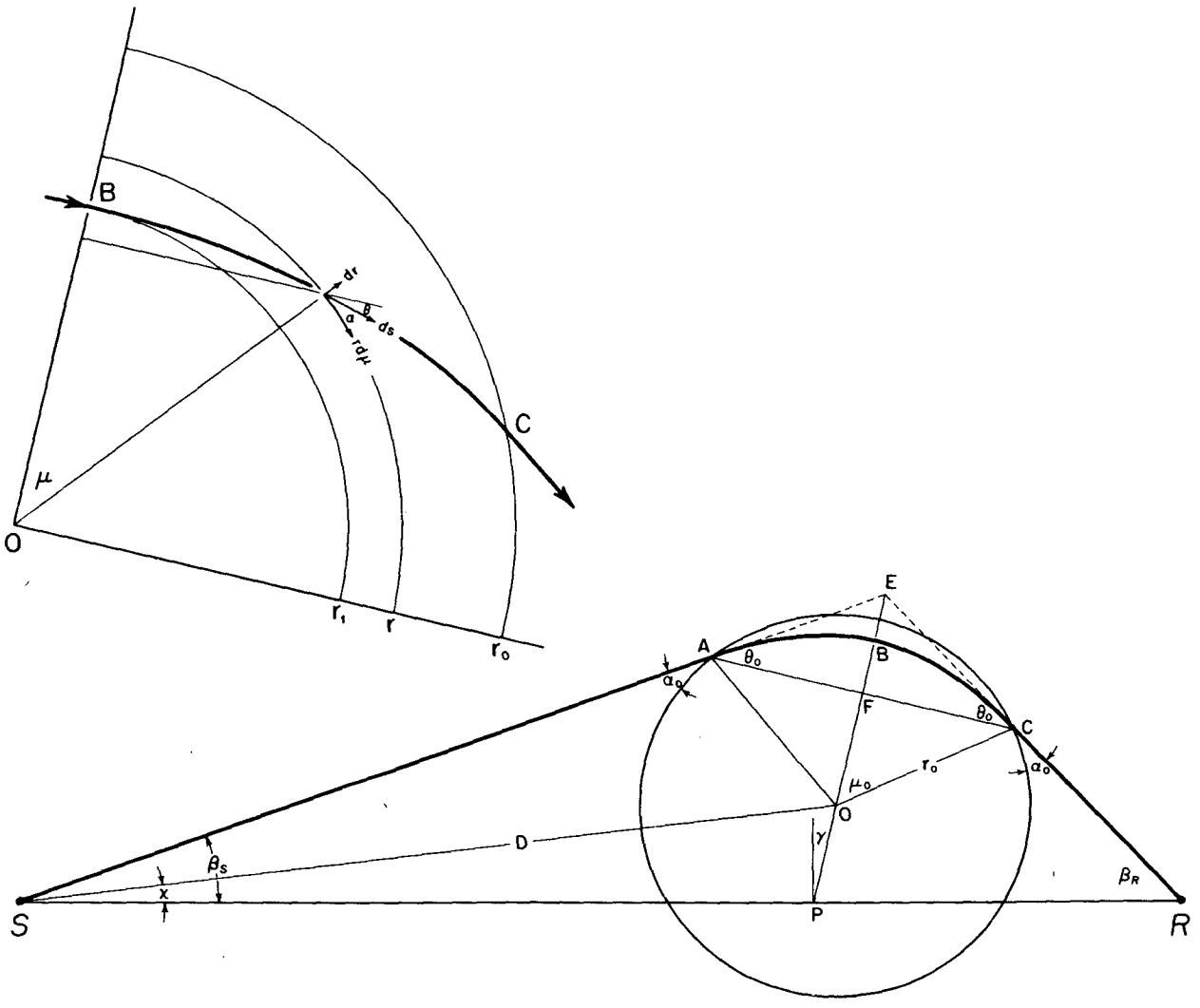

FIG. 1. Ray path S-A-B-C-R from a source S(0,0) to a receiver R(R,0) through a cold eddy of radius r_0 centered at O($D\cos\chi$, $D\sin\chi$). The ray path through the eddy is shown on an enlarged scale to the upper left; B with polar coordinates $r = r_1$, $\mu = 0$ is the ray midpoint inside the eddy, and C(r_0,μ_0) is the exit point. The ray forms an angle α relative to the local r circle, and θ with respect to its direction at the midpoint B; thus $\mu = \alpha + \theta$.

$$n = 1 + \nu\left(1 - \frac{\cos\alpha_0}{\cos\alpha}\right) + O(\nu^2),$$

$$\frac{dn}{n} = -\nu\cos\alpha_0 \sec\alpha \tan\alpha d\alpha + O(\nu^2).$$

Substituting this into Eq. (4) gives an exit angle

$$\theta_0 = \nu\cos\alpha_0 \int_0^{\alpha_0} \sec\alpha d\alpha$$

$$= \nu\cos\alpha_0 \cosh^{-1}(\sec\alpha_0). \qquad (6)$$

For grazing incidence, $\alpha_0 \ll 1$, and

$$\theta_0 = \nu\alpha_0 \to 0 \quad \text{as} \quad \alpha_0 \to 0.$$

For normal incidence, $\alpha_0 \approx \frac{1}{2}\pi$, and

$$\theta_0 = \nu\cos\alpha_0 \ln\frac{2}{\cos\alpha_0} \to 0 \quad \text{as} \quad \alpha_0 \to \tfrac{1}{2}\pi.$$

There is a maximum deflection when $\cosh(\csc\alpha_0) = \sec\alpha_0$ or $\alpha_0 = 0.985$. This equals

$$(\theta_0)_{\max} = \nu/\tan\alpha_0 = 0.664\nu.$$

Thus, the rays that suffer the most deflection penetrate to within a fraction $r_1/r_0 \approx \cos\alpha_0 = 0.553$ of the eddy radius.

These results are not too sensitive to the assumed model:

Model	$n(r \leq r_0)$	(θ_0) maximum
A	$1 + \nu \frac{r_0 - r}{r_0}$	0.664ν at $r_1/r_0 = 0.553$
B	$1 + \nu \frac{r_0^2 - r^2}{r_0^2}$	ν at $r_1/r_0 = 0.707$
C	$1 + \nu \left(\frac{r_0^2 - r^2}{r_0^2}\right)^2$	0.699ν at $r_1/r_0 = 0.303$.

We shall use model B for its simplicity. It gives the general result

$$\theta = \nu \sin 2\alpha, \tag{7}$$

where we have now written θ, α for θ_0, α_0.

4. Deflection

For a specified eddy location and radius there are restrictions on θ and α in order for the rays to reach the receiver (Fig. 1). These are derived in the Appendix. For the special case of an eddy at equal distance from transmitter and receiver, with its center at a distance Y from the line between transmitter and receiver, we have for small θ

$$Y/r = (\sigma \sin\alpha - 1)\cos\alpha, \quad \sigma = \nu R/r. \tag{8}$$

The simple equations (7) and (8) contain the vital information for a variety of situations, depending upon which of the four ranges, A, B, C, D is occupied by σ:

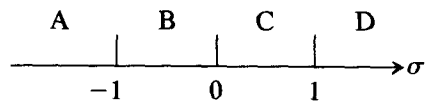

This is illustrated in Fig. 2. Take the case of a weak, cold eddy, with $\nu = +0.01$, $R = 1000$ km, $r = 100$ km and $\sigma = +0.1$ (Fig. 3). As the eddy first comes into line-of-sight from the left, the ray is sharply deflected to the right (away from the eddy center), soon reaching a maximum deflection $\theta = \nu$. It drifts back to the undisturbed direction as the eddy is centered, etc. There is only one ray path provided $\sigma < 1$. For $\sigma > 1$ there can be one or three separate arrivals, depending on the eddy location. For warm eddies the deflection is opposite in direction (toward the eddy center), and there are multipaths even for weak eddies when the eddy is just beyond the line of sight (but not otherwise).

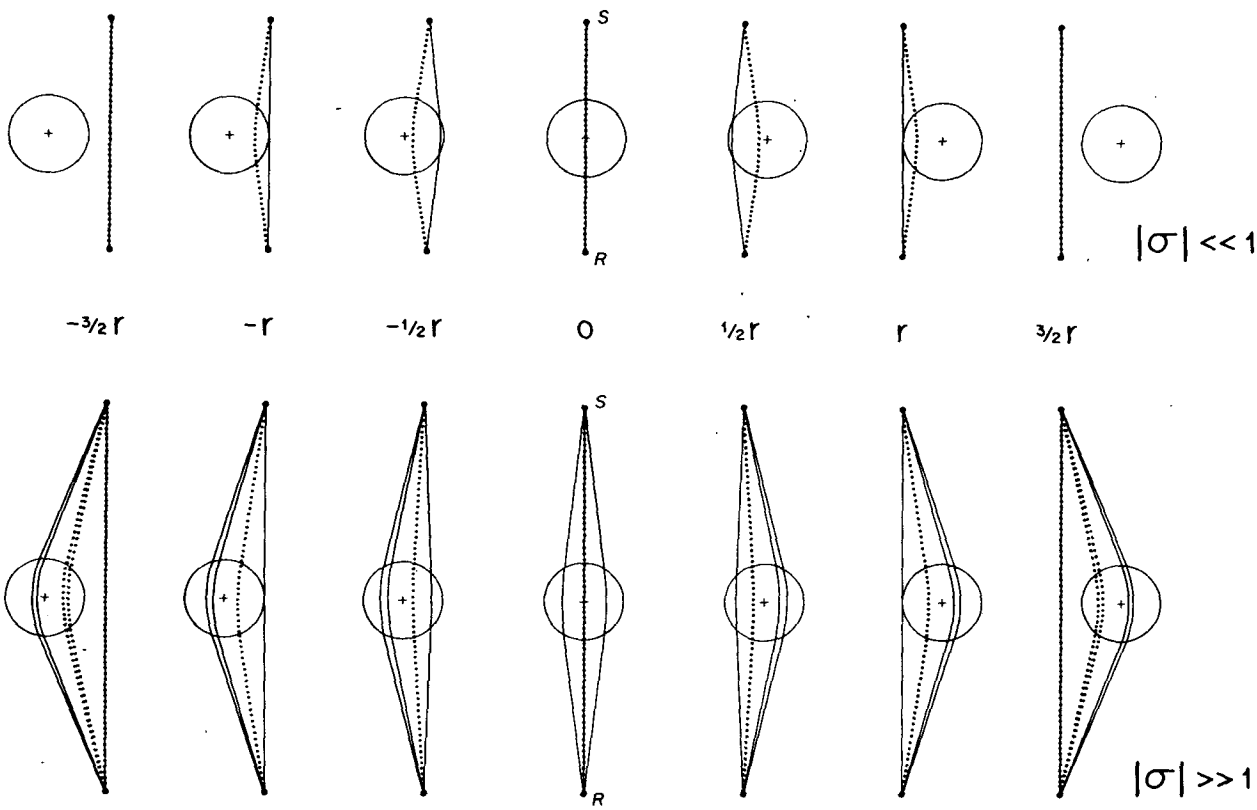

FIG. 2. Deflection of paths by cold (solid) and warm (dotted) eddies, or both (dash-dotted). The eddy moves from left to right as seen by an observer at the receiver R looking toward the source S. The upper seven panels refer to short ranges $R \ll r/|\nu|$ and the lower panels to long ranges $R \gg r/|\nu|$ (for a fixed eddy radius r and velocity defect $|\nu|$). For the short ranges (which is the usual situation) the apparent source direction at the receiver is deflected toward the eddy center for warm eddies, and away from the eddy center for cold eddies. There is only a single path, and the eddy has no effect once it is outside the line of sight. For long ranges (or small intense eddies) there are multiple paths and these can persist for some distance outside the line of sight, as can be seen in the lower panels.

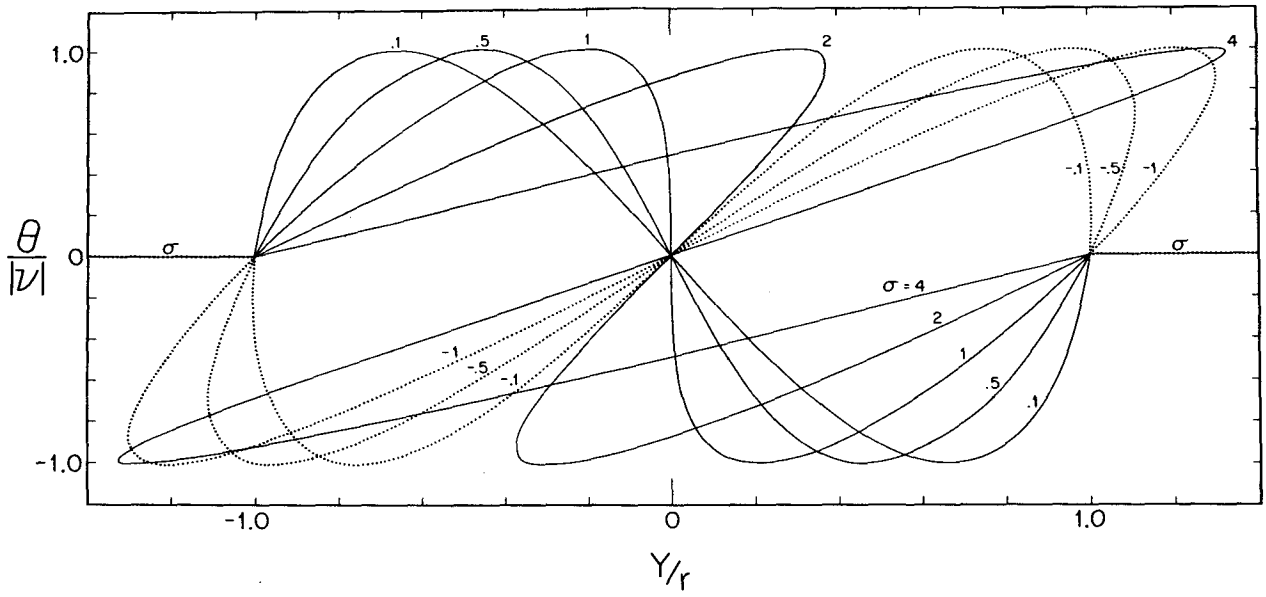

FIG. 3. The angular deflection $\theta/|\nu|$ of the incoming rays as a function of the eddy displacement Y/r, for stated values of $\sigma = \nu R/r$. Positive σ (solid) corresponds to cold eddies, negative σ (dotted) to warm eddies.

5. Intensity

We now consider a small change in the source azimuth, from β_S to $\beta_S + \delta\beta_S$, other factors remaining fixed (Fig. 1). As a result the ray intersects the line SPR (Fig. 1) at a range $R + \delta R$. The distance between the two differential rays is $\delta R \sin\beta_R$. If there is no eddy, this distance is $R\delta\beta_S$. The ratio

$$I = \left| \frac{R\delta\beta_S}{\sin\beta_R \delta R} \right| \tag{9}$$

is then a measure of relative intensity.

For the special case of an eddy equidistant from transmitter and receiver, we find (Appendix)

$$I = \left| \frac{\sin\alpha}{\sin\alpha + \sigma \cos 2\alpha} \right| . \tag{10}$$

which has been plotted against Y and σ (Fig. 4) with the help of (7) and (8).

The strongest signal from a warm eddy is just before it comes into the line of sight; whereas for a cold eddy the intensity drops sharply just after it comes into the line of sight. When the eddy is cen-

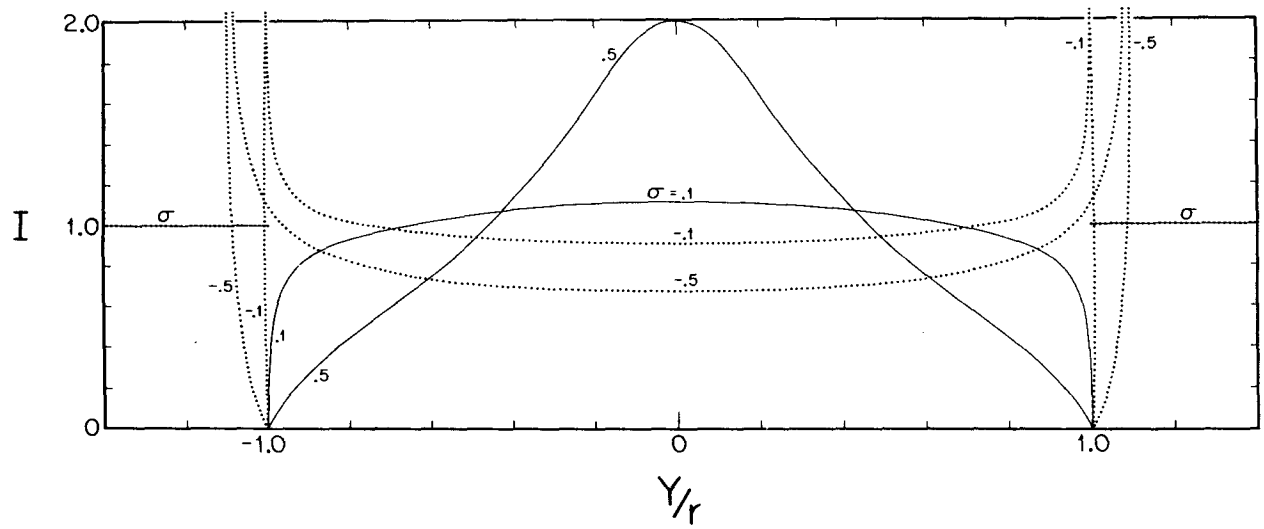

FIG. 4. The relative intensity for cold eddies (solid, $\sigma > 0$) and warm eddies (dotted, $\sigma < 0$), or both (dash-dotted). For warm eddies, the intensity is a maximum when the eddy is just beyond the line of sight ($|Y|/r = 1 + \epsilon$) and a minimum when it is centered on the line of sight ($Y = 0$); for cold eddies the intensity is a minimum when the eddy is just inside the line of sight ($|Y|/r = 1 - \epsilon$) and a maximum when it is centered.

tered between source and receiver, the intensity is $(1 - \sigma)^{-1}$ and so is enhanced for cold eddies and diminished for warm eddies.

6. Travel times

We first take the travel time within the eddy

$$\int \frac{[(dr)^2 + (rd\mu)^2]^{1/2}}{C(r)} = \int \frac{dr}{C(r)\sin\alpha} = \frac{1}{C_0}\int \frac{rn}{\sin\alpha}\frac{dr}{r}.$$

Using Snell's law, $\sec\alpha = rn/r_0 \cos\alpha_0$, and its total differential, this can be written

$$\frac{2r_0\cos\alpha_0}{C_0}\left[\int_0^{\alpha_0}\sec^2\alpha d\alpha - \int_{n(r_1)}^{1}\frac{1}{\sin\alpha\cos\alpha}\frac{dn}{n}\right] = \frac{2r_0}{C_0}\sin\alpha_0[1 + \omega],$$

$$\omega = \frac{-1}{\tan\alpha_0}\int_{n(r_1)}^{1}\frac{1}{\sin\alpha\cos\alpha}\frac{dn}{n}.$$

For the special case of model B,

$$\frac{dn}{n} = -\frac{2\nu\sec^2\alpha\tan\alpha}{\sec^2\alpha_0}\,d\alpha,$$

$$\omega = \tfrac{2}{3}\nu(1 + 2\cos^2\alpha_0).$$

The travel time outside the eddy is $SA/C_0 + CR/C_0$ (Fig. 1). We subtract R/C_0 to obtain the travel time excess

$$\tau = \frac{SA + CR - R}{C_0} + \frac{2r\sin\alpha}{C_0}(1 + \omega). \quad (11)$$

(Again the subscripts 0 have been dropped from r, α.) After some rather tedious geometry (Appendix), we find for the previous example

$$\tau = (\nu r/C_0)2\sin^2\alpha(\tfrac{2}{3}\sin\alpha + \sigma\cos^2\alpha). \quad (12)$$

Thus, τ scales as $\nu r/C_0 = O(1\text{ s})$, as expected. It properly vanishes for $\nu = 0$ and for $r = 0$; it also vanishes for glancing incidence, $\alpha = 0$, and for $\sigma = -\frac{2}{3}\sin\alpha\sec^2\alpha$, when the additional eddy path length is just balanced by the increased speed in a warm eddy. τ is always positive for a cold eddy (positive ν and positive $\sigma = \nu R/r$).

For small σ, the extremum for τ is for head-on incidence, $\alpha = 90°$, and equals (4/3) $\nu r/C_0$. For large σ, τ is a maximum when $\alpha = 45°$, and amounts to $\frac{1}{2}\sigma\nu r/C_0$.

In the usual application of perturbation analysis, one interprets variations in travel time in terms of variations in sound speed along the *unperturbed* path (e.g., Munk and Wunsch, 1979). We can now interpret the implication of this approximation. The travel-time excess along the unperturbed path, that is, along the straight line from transmitter to receiver entering the eddy at x_1 and exiting at x_2, is given by

$$\tau_u = \int_{x_1}^{x_2}\frac{dx}{C(x)} - \frac{x_1 - x_2}{C_0}.$$

This turns out to be identical with the term involving $\frac{2}{3}\sin\alpha$ in Eq. (12). The correction for path perturbation is thus of order σ. The calculations of travel time along the unperturbed path make no sense when $\sigma > 1$; as an example, $\tau_u = 0$ when the eddy is outside the line of sight, yet there can be delayed arrivals through the eddy.

7. Mesoscale eddies

For a typical mesoscale eddy, we take a temperature anomaly of $\delta\theta = 3°C$. This causes a fractional change in sound speed of $\delta C/C = -\nu \approx 10^{-2}$. The horizontal deflection is $\sim|2\nu|$ or 1°. The parameter $\sigma = \nu R/r = 0.1$ for $r = 100$ km, $R = 1000$ km.

The emphasis here has been on isolated eddies. For mesoscale eddies a more meaningful viewpoint might be a random field. We can use the present results for guidance by considering the random walk problem with a typical scattering "event" for each $2r \approx 200$ km. Then for a 1000 km range the horizontal deflection needs to be multiplied by $5^{1/2}$.

We have discussed the problems of horizontal refraction as if the ray paths remained in a fixed horizontal plane, in order to avoid the complexities of the three-dimensional refraction problem. I believe this procedure is a reasonable way to get at the magnitudes involved, but it will eventually have to be tested by a three-dimensional treatment. Quite apart from this problem there is a question as to the variations with depth of the horizontal gradients.

Let $\eta(z)$ designate the upward displacement of water at the eddy center. η can be of either sign

Cold eddy	Warm eddy
Cyclonic	Anticyclonic
η, ν, σ positive	η, ν, σ negative
δC negative	δC positive.

For a rough guidance, we can use linear theory (Andrews and Scully-Power, 1976; Richman *et al.*, 1977) to obtain

$$\frac{d^2\eta}{dz^2} + \frac{N^2(z)}{c^2}\eta = 0, \quad (13)$$

where N is the buoyancy frequency and c a separation constant so determined that $\eta = 0$ at the surface and bottom. The WKB solution is

$$\eta \approx N^{-1/2}\exp[\pm ic^{-1}\int N dz].$$

We now consider an exponentially stratified ocean, $N = N_0 e^{z/B}$; the stratification scale B is of order 1 km and does not vary greatly from top to bottom (Garrett and Munk, 1972). Then $\int N dz = BN(z)$ and for constant B

$$\eta(z) \approx N^{-1/2}(z) \sin\left[j\pi \frac{N_0 - N(z)}{N_0 - N_b}\right], \quad j = 1, 2, \ldots,$$

satisfies the boundary conditions with N varying from a maximum value N_0 near the surface to $N_b \ll N_0$ near the bottom. We shall be concerned only with the lowest mode, $j = 1$, which contains most of the energy (Richman *et al.*, 1977). Then for a maximum displacement of approximately A, we have

$$\eta(z) = 2^{-1/2} A \frac{N_0^{1/2}}{N^{1/2}(z)} \sin\left[\pi \frac{N_0 - N(z)}{N_0 - N_b}\right]. \quad (14)$$

(The WKB approximation is rather poor for $j = 1$.) The maximum displacement, $\eta \approx A$, occurs near a depth, where $N(z) = \frac{1}{2}N_0$.

The index of sound refraction is written

$$n = 1 + \nu(z), \quad \nu = \frac{1}{C}\frac{\partial C_p}{\partial z}\eta(z), \quad (15)$$

where

$$\frac{1}{C}\frac{\partial C_p}{\partial z} = \frac{1}{C}\frac{\partial C}{dz} - \kappa$$

is the *potential* fractional sound speed gradient, and $\kappa = -1.4 \times 10^{-5}\ \mathrm{m}^{-1}$ is the corresponding adiabatic gradient. At the axis, $\partial_z C$ vanishes and $C^{-1}\partial_z C_p = -\kappa$. In an isohaline ocean the gradients of potential sound speed and potential density are roughly proportional, and we can write

$$C^{-1}\partial_z C_p = (-\kappa)N^2(z)/N_1^2, \quad (16)$$

where N_1 is the buoyancy frequency at the sound axis. In the presence of a salinity gradient equation (16) can still serve as a rough guide (Flatté *et al.*, 1979).

The excess in the index of sound refraction at the eddy center is then

$$\nu(z) = 2^{-1/2} A(-\kappa) \frac{N^{3/2}(z)}{N_1^2 N_0^{-1/2}} \times \sin\left[\pi \frac{N_0 - N(z)}{N_0 - N_b}\right]. \quad (17)$$

Table 1 gives some selective estimates with a maximum displacement $A = 100$ m; the maximum vertical displacement is at 700 m depth and the maximum index of refraction is at 350 m. In order to obtain $\nu = 0.01$ as used for earlier estimates, a maximum displacement of ~300 m would be required. ν is very small at great depth.

TABLE 1. Vertical displacement η and the associated excess ν in the index of refraction at the center of a cold eddy for $j = 1$. The maximum vertical displacement is taken as $A = 100$ m. Maximum values in italics.

	Depth (m)	N (cph)	η (m)	ν
Near surface	100	3	0	0
	200	2.5	42	3.0×10^{-3}
	300	2.1	72	*3.7×10^{-3}*
	400	2	79	3.6×10^{-3}
	700	1.5	*100*	2.5×10^{-3}
Sound axis	1000	1.0	53	1×10^{-3}
	2000	0.5	49	1×10^{-4}
Bottom	4500	0.25	0	0

8. Gulf Stream rings

The most intense eddies are formed by instabilities of the western boundary currents. These have been intensively studied off the Gulf Stream and the East Australia Current. On the continental side of the Gulf Stream the eddies have a core of warm Sargasso water, on the seaward side a core of cold slope water. There are certain dynamic restraints imposed on these eddies, and these restraints differ somewhat for the warm and cold eddies. What are the implications with regard to the parameters ν and σ?

It has been found (Andrews and Scully-Power, 1976; Csanady, 1979; Flierl, 1979) that the Gulf Stream rings can be roughly characterized by constant potential vorticity. For the simplest case of radially symmetric motion confined to an upper layer of thickness $h(r)$ we have

$$\frac{(dv/dr) + (v/r) + f}{h} = \frac{f}{H}. \quad (18)$$

Here H is the undisturbed layer thickness, and $\eta(r) = H - h(r)$ is the upward displacement of the internal boundary; $v(r)$ is the azimuthal velocity. Eq. (18), together with the geostrophic assumption

$$v = \frac{g'}{f}\frac{dh}{dr}, \quad g' = g\frac{\Delta\rho}{\rho} \quad (19)$$

(thus ignoring v^2/r as compared to the Coriolis force fv), leads to the Bessel equation

$$\frac{d^2\eta}{dx^2} + \frac{1}{x}\frac{d\eta}{dx} - \eta = 0, \quad x = \frac{r}{r_d},$$

where

$$r_d = (g'H)^{1/2}/f \quad (20)$$

is the Rossby radius of deformation.

For a warm eddy, the appropriate solution is

$$\eta(r) = H\frac{I_0(r/r_d)}{I_0(r_0/r_d)}, \quad v(r) = -r_d f\frac{I_1(r/r_d)}{I_0(r_0/r_d)}, \quad r \leqslant r_0. \tag{21}$$

The warm core is bounded by $r = r_0$ (Fig. 5); at the eddy center the depth of the warm core is

$$h(0) = H - \eta(0) = H[1 - I_0^{-1}(r_0/r_d)].$$

We may interpret the present two-layer model as the case of continuous stratification; the variation ν in the index of refraction between eddy center and the outlying water is then proportional to $h(0)$ and so increases indefinitely with increasing r_0. On the other hand, the parameter $\sigma = \nu R/r_0$ has a maximum value for $r_0 \approx 2r_d$ (Table 2).

To take some numerical values, we set

$$g' = 10^{-2}\ \text{m s}^{-2}, \quad H = 1000\ \text{m},$$
$$f = 0.8 \times 10^{-4}\ \text{s}^{-1};$$

hence,

$$r_d = 40\ \text{km}, \quad r_d f = 3.2\ \text{m s}^{-1}.$$

For an extreme 9°C differential between the warm core and surrounding cold water, $\nu = -0.03$, so that $\theta \approx 4°$. The largest magnitude of σ occurs when $r_0 = 2r_d = 80$ km, giving $\sigma = -0.4$.

For cold rings

$$\left.\begin{aligned} \eta(r) &= H\frac{K_0(r/r_d)}{K_0(r_0/r_0)}, \\ v(r) &= r_d f\frac{K_1(r/r_d)}{K_0(r_0/r_d)}, \\ r &> r_0 \end{aligned}\right\}, \tag{22}$$

and $\nu \approx \eta(r_0) - \eta(\infty) = H$, independent of r_0. Thus σ increases indefinitely with decreasing r_0, but for small r_0 the velocities become unrealistically large. The maximum flow is just outside r_0, and equals 1.43 $r_d f$ for $r = r_0$ and 1.23 $r_d f$ for $r = 2r_0$ (Table 2). The scaling velocity $r_d f = 3.2$ m s^{-1} is too high because of the neglect of the cyclostrophic term v^2/r (Flierl, 1979), but even so it is doubtful whether cold rings can have radii much smaller than $r_0 = 2r_d$, and we are back to the same numerical values as for the warm ring.

We have not yet considered the role played by the currents in deflecting the acoustic rays. This is of order $v/C \approx 10^{-3}$ for intense rings, and small compared to $-\nu = \delta C/C \approx 10^{-2}$ from the vertical

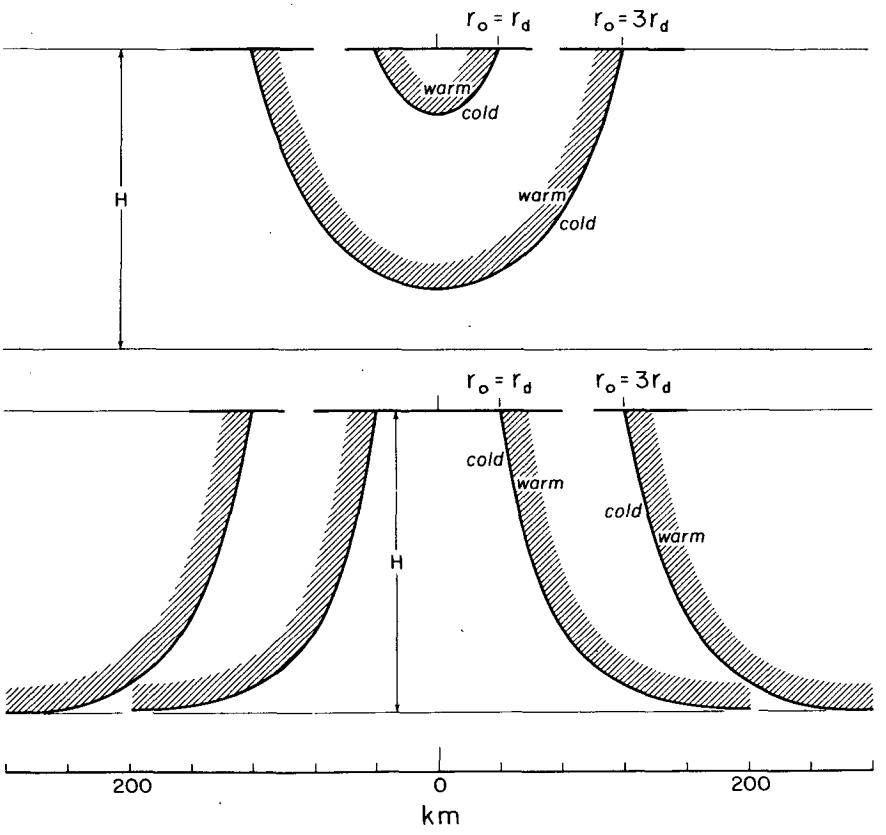

FIG. 5. Warm and cold core rings of constant potential vorticity for the two cases $r_0 = r_d$ and $r_0 = 3r_d$, where $r_d \approx 40$ km is the Rossby radius of deformation (from Csanady, 1979).

TABLE 2. Parameters of warm and cold core rings with constant potential vorticity for various eddy sizes: 1) is the relative vertical displacement of the interface, 2) is a fraction proportional to the parameter σ, and 3) is the radial velocity at the perimeter r_0 (where it is largest), in units of $r_d f \approx 3$ m s^{-1}.

$r_0/r_d =$	1	2	3	4	5
		Warm core			
1) $[(\eta(r_0) - \eta(0))/H]$	0.21	0.56	0.80	0.91	0.96
2) $(r_0/r_d)^{-1}$[above]	0.21	0.28	0.27	0.23	0.19
3) $v(r_0)/r_d f$	−0.45	−0.70	−0.81	−0.86	−0.89
		Cold core			
1) $[(\eta(r_0) - \eta(\infty))/H]$	1	1	1	1	1
2) $(r_0/r_d)^{-1}$[above]	1	0.50	0.33	0.25	0.20
3) $v(r_0)/r_d f$	1.43	1.23	1.16	1.12	1.10

displacements of the isotherms. The relative magnitude reverses at abyssal depths, but there the refraction by currents and by vertical displacements are both negligible.

9. Discussion

We have introduced the concept of an eddy focal length r/ν. For weak eddies this is of order 10 000 km, whereas for intense Gulf Stream rings this might be as small as 2000 km.[1] Certain simplifications occur if the acoustic range is within the eddy focal length, as will usually be the case. Under such circumstances the ray paths will be horizontally deflected by a few degrees, but they will not be split into horizontal multipaths. This implies that the horizontal deflection could be measured by interferometry using two receivers separated by something like 10 acoustic wavelengths. (A dense array would be required to resolve multipaths.)

The incoming ray, in addition to being deflected by mesoscale disturbances in the oceans, will be broadened by ocean finestructure. For internal wave-induced finestructure, the horizontal mean-square spread is [Flatté *et al.*, Eq. (13.4.4)] $10^{-11} \times [N(z)/N(-B)]^3$ rad^2 m^{-1}, or 0.003 rad rms at 1000 km for the axial ray, 0.01 rad for steep rays. The internal wave-induced spread is then of the same order as the mesoscale-induced deflection. In principle, it is still possible to measure the mesoscale-induced deflection by averaging transmissions over time scales large compared to internal wave time scales of a day, but small compared to mesoscale time scales of several months.

Acknowledgments. I am indebted to Peter Worcester and Robert Knox for suggesting some changes and to a reviewer for pointing out a number of errors and suggesting improvements. The Office of Naval Research has supported this work.

[1] There appear to be some fundamental dynamic considerations which impose a limit on both the eddy radius and its intensity, and hence on r/ν. An analysis of Scully-Power (1979) based largely on the work of Rhines (1976) suggests $r/\nu = O[g'/(\epsilon N f)] \approx 2000$ km, where $\epsilon \approx 10^{-2}$ is the fractional adiabatic increase in sound speed over a scale depth.

APPENDIX

Acoustic Paths for Cylindrical Symmetry

1. Snell's Law

We start with Fermat's principle $\delta T = 0$ in cylindrical coordinates (Fig. 1):

$$T = \int \frac{[(dr)^2 + (rd\mu)^2]^{1/2}}{C(r)} = \int_0^{\mu_0} \mathcal{L} d\mu,$$

with

$$\mathcal{L} = (r'^2 + r^2)^{1/2}/C(r), \quad r' = dr/d\mu.$$

The integrand $\mathcal{L}$ does not depend explicitly on μ, and accordingly the Hamiltonian is a constant:

$$H = r' \frac{\partial \mathcal{L}}{\partial r'} - \mathcal{L} = C^{-1}[r'^2(r^2 + r'^2)^{-1/2} - (r^2 + r'^2)^{1/2}]$$

$$= -C^{-1}r^2(r^2 + r'^2)^{-1/2} = -C_0^{-1}\mathrm{nr}[1 + (r'/r)^2]^{-1/2},$$

where $n(r) = C_0/C(r)$ is the index of refraction referred to conditions outside the eddy. But $r'/r = \tan\alpha$, where α is the angle between the ray path $r(\mu)$ and the local tangent to the circular n contours. Thus we have Snell's law [Eq. (2)].

2. Path geometry

A ray S-A-B-C-R travels from source S(0,0) to receiver R(0,R), with A-B-C being the portion within the eddy (Fig. 1). For simplicity, source and receiver are assumed outside the eddy. (We can now drop the subscripts 0 for referring to conditions at the eddy boundary.) Thus α ($=\alpha_0$) is the incidence angle at A between the ray and the outer eddy contour, and also the exit angle at B; α varies from 0 for grazing incidence to 90° at normal impact. The ray suffers a total deflection of 2θ. Conditions of symmetry give

$$\beta_S = \theta - \gamma, \quad \beta_R = \theta + \gamma. \tag{A1,2}$$

We require that the bisector E-B-F-O-P go through the eddy center O(X, Y):

$$\tan\gamma = (X - \mathrm{SP})/Y. \tag{A3}$$

From the triangles S-E-P and R-E-P we have

$$\frac{\sin\beta_S}{\mathrm{PE}} = \frac{\sin(90 - \theta)}{\mathrm{SP}}, \quad \frac{\sin\beta_R}{\mathrm{PE}} = \frac{\sin(90 - \theta)}{\mathrm{PR}},$$

and so, with PR $= R -$ SP

$$\frac{\sin\beta_S}{\sin\beta_R} = \frac{R - \mathrm{SP}}{\mathrm{SP}}. \tag{A4}$$

Eliminating SP between (A3) and (A4), and using (A1,2),

$$\tan\gamma = \frac{X - \tfrac{1}{2}R}{Y + \tfrac{1}{2}R\cot\theta}. \tag{A5}$$

We require a relation between α and θ. We have not yet used the known eddy radius. From triangle S-O-A we have

$$\frac{\sin(\beta_S - \chi)}{r} = \frac{\sin(90 + \alpha)}{D}, \quad D = \mathrm{SO}$$

or

$$r\cos\alpha = X\sin(\theta - \gamma) - Y\cos(\theta - \gamma). \tag{A6}$$

Eqs. (A1), (A2), (A5) and (A6) together with the relation $\theta(\alpha)$ for a given refractive model provide five equations to solve for β_S, β_R, θ, α, γ for a given R, X, Y. We are concerned with small values of θ. Then $\gamma \approx \theta(2X/R - 1) \ll 1$, and so

$$\frac{Y}{r} \approx \frac{2X}{r}\left(1 - \frac{X}{R}\right)\theta - \cos\alpha. \tag{A7}$$

For the special case $X = \tfrac{1}{2}R$ and refractive model B, this reduces to Eq. (8).

3. Intensity

The problem is to evaluate Eq. (9). Generally

$$\delta\beta_S = \delta\theta - \delta\gamma. \tag{A8}$$

For small θ, it follows from (A7) that $\gamma = \theta(2X/R - 1)$ and so

$$\delta\gamma = \delta\theta(2X/R - 1) - \theta(2X/R^2)\delta R. \tag{A9}$$

Differentiation of Eq. (A7) gives

$$0 = \frac{2X}{r}\left[\left(1 - \frac{X}{R}\right)\delta\theta + \frac{X}{R^2}\theta\delta R\right] + \sin\alpha\delta\alpha. \tag{A10}$$

For refractive model B, $\theta = \nu\sin 2\alpha$, and so

$$\delta\theta = 2\nu\cos 2\alpha\delta\alpha. \tag{A11}$$

We have four equations relating $\delta\beta_S$, $\delta\theta$, $\delta\gamma$, δR and $\delta\alpha$, which can be solved for the ratio $\delta\beta_S/\delta R$. The result is

$$I = \left|1 + 4\left(1 - \frac{X}{R}\right)\frac{\nu X\cos 2\alpha}{r\sin\alpha}\right|^{-1}. \tag{A12}$$

This reduces to Eq. (10) for $X = \tfrac{1}{2}R$.

4. Travel time

The problem is to evaluate Eq. (11)

$$\tfrac{1}{2}\tau C_0 = \tfrac{1}{2}(\mathrm{SA} + \mathrm{CR} - R) + r(1 + \omega)\sin\alpha$$

with

$$\omega = \tfrac{2}{3}\nu(1 + 2\cos^2\alpha).$$

After some tedious geometry, we find

$$\mathrm{SA} = X\cos(\theta - \gamma) + Y\sin(\theta - \gamma) - r\sin\alpha,$$

$$\mathrm{CR} = X\cos(\theta + \gamma) + Y\sin(\theta + \gamma) - r\sin\alpha,$$

so that

$$\tfrac{1}{2}\tau C_0 = X\cos\gamma\cos\theta + Y\cos\gamma\sin\theta - \tfrac{1}{2}R + \omega\sin\alpha.$$

For the special case $X = \tfrac{1}{2}R$, hence $\gamma = 0$, we have, to second order in $\theta = \nu\sin 2\alpha$,

$$\tfrac{1}{2}\tau C_0 = -\frac{r\sigma}{4\nu}\theta^2 + r\cos\alpha(\sigma\sin\alpha - 1)\theta + \tfrac{2}{3}r\nu\sin\alpha(1 + 2\cos^2\alpha) = \nu r\sin^2\alpha(\tfrac{2}{3}\sin\alpha + \sigma\cos^2\alpha)$$

in agreement with Eq. (12).

REFERENCES

Andrews, J. C., and P. Scully-Power, 1976: The structure of an East Australian Current anticyclonic eddy. *J. Phys. Oceanogr.*, **6**, 756–765.

Csanady, G. T., 1979: The birth and death of a warm core ring. *J. Geophys. Res.*, **84**, 777–780.

Flatté, S. M. (Ed.), R. Dashen, W. H. Munk, K. M. Watson and F. Zachariasen, 1979: *Sound Transmission Through a Fluctuating Ocean*. Cambridge University Press, 299 pp.

Flierl, G. R., 1979: A simple model for the structure of warm and cold core rings. *J. Geophys. Res.*, **84**, 781–785.

Garrett, C. J. R., and W. H. Munk, 1972: Space-time scales of internal waves. *Geophys. Fluid Dyn.*, **2**, 225–264.

Harrison, C. H., 1977: Three-dimensional ray paths in basins, troughs, and near seamounts by use of ray invariants. *J. Acoust. Soc. Amer.*, **62**, 1382–1388.

Munk, W., and C. Wunsch, 1979: Ocean acoustic tomography: a scheme for large scale monitoring. *Deep-Sea Res.*, **26A**, 123–161.

Rhines, P. B., 1976: The dynamics of unsteady currents. *The Sea*, Vol. 6, Wiley-Interscience, 189–318.

Richman, J. G., C. Wunsch and N. Hogg, 1977: Space and time scales of mesoscale motion in the western North Atlantic. *Rev. Geophys. Space Phys.*, **15**, 385–420.

Scully-Power, P., 1979: Mesoscale inhomogeneities and turbulence in ocean acoustics. *Cavitation and Inhomogeneities in Underwater Acoustics*, W. Lauterborn, Ed., Vol. 4, *Springer Series in Electrophysics*, Springer-Verlag, 294–307.